Solar Energy Materials and Solar Cells 185 (2018) 192–197

Contents lists available at ScienceDirect

Solar Energy Materials and Solar Cells

journal homepage: www.elsevier.com/locate/solmat

Temperature effects of bifacial modules: Hotter or cooler?

M.W.P.E. Lamers[a], E. Özkalay[a], R.S.R. Gali[a], G.J.M. Janssen[a], A.W. Weeber[a,b], I.G. Romijn[a], B.B. Van Aken[a,*]

[a] ECN part of TNO – Solar Energy, Westerduinweg 3, 1755 LE Petten, The Netherlands
[b] Delft University of Technology, PVMD Group, Mekelweg 4, 2628 CD Delft, The Netherlands

ARTICLE INFO

Keywords:
Bifacial PV module
Outdoor performance
Bifacial efficiency
Operating temperature
Thermal behaviour

ABSTRACT

In this paper we show the results from indoor and outdoor measurements on solar cells and modules, manufactured with different bifacial and monofacial cell architectures and encapsulated in different configurations. Reflection/transmission, IV and IQE spectra of single-cell laminates were measured and used to determine the energy spectra for all heat loss and absorption processes, including thermalisation, recombination, entropy generation, parasitic absorption and electrical power generation. From these spectra, the effective heat input was calculated for front, rear and combined irradiance. The power output, bifacial gain and module operating temperature were monitored of single-cell laminates exposed to indoor irradiance as well as of full-size modules installed on our rooftop.

We have found that the effective heat input for bifacial glass-glass modules is increasingly larger with increasing rear irradiance compared to monofacial modules. Measured temperatures of rooftop-installed modules strongly indicate that the effective heat transfer coefficient of glass-glass modules is higher than that of white back sheet modules. The observed combined effect of heat input and heat transfer is that only at rear irradiance fractions beyond 15% the additional heat input can cause the bifacial modules to be hotter than their monofacial counterpart, but the energy yield is still much higher due to the large bifacial gain. In the case of moderate albedo, the bifacial energy gain is not accompanied by a higher temperature of the bifacial module compared to the monofacial module.

1. Introduction

Bifacial cells and modules collect light falling on the front-side of the panels, but also collect light falling on the rear. This will increase the total irradiance absorbed by the panel, and the current generated by the panels increases accordingly. One of the remaining research questions is whether bifacial solar panels operate at higher or at lower temperatures than monofacial panels. One side of the argument is that the extra light absorption increases the module temperature, which will negatively affect the total power output of the panels and reduce the effective bifacial yield gain. On the other hand, as the infrared (IR) light transmission through the panels is also higher [1], it can be argued that the panels will be cooler. Also, Hezel showed that in a bifacial PV panel with about one cell's width spacing between the bifacial solar cells, the temperature is lower compared to densely packed monofacial module [2]. Excess heat has a negative effect on the power output of photovoltaic (PV) modules, as the V_{oc} decreases with increasing solar cell temperature [3,4]. Optoelectric properties of the cell and the module materials are critical parameters for the module temperature under operating conditions. The heat balance in a PV module is affected by three main factors: i) irradiance that is absorbed, transmitted or reflected; ii) conversion losses either by thermalisation, entropy generation, recombination or parasitic absorbance [5,6] and iii) heat losses by radiation and convection. The irradiance that enters the cell is absorbed or transmitted through the cell. The light that is transmitted through a cell, mostly (near-)IR light, is either transmitted out of the module, absorbed by the module materials or reflected back to the cell. Module materials are, for example, polymer back sheet or rear glass panel. The irradiance absorbed by the cell will be partly used to produce electricity but will also produce heat due to the conversion losses, described above.

In this work we will show the contribution of these thermal processes to the heat balance and the actual (working) temperature of the module. First, we analyse the spectral dependence of the optical and electrical behaviour of different solar cell architectures and single-cell laminates in laboratory. Then, the effective heat input is determined. The heat transfer coefficient is determined for monofacial and bifacial modules under controlled indoor conditions. Also, the effect of

* Corresponding author.
E-mail address: bas.vanaken@tno.nl (B.B. Van Aken).

https://doi.org/10.1016/j.solmat.2018.05.033
Received 19 March 2018; Received in revised form 14 May 2018; Accepted 15 May 2018
0927-0248/

additional rear illumination on the overall heat balance of the different single-cell laminates is presented. Subsequently, we analyse outdoor data of the single-cell laminates and confirm the results by a comparison with commercial modules on a flat rooftop.

2. Experimental section

Monofacial white back sheet and bifacial glass-glass single-cell laminates were manufactured; both types of modules were made with monofacial Al-BSF and with bifacial n-PERT solar cells. The Al-BSF solar cell is the conventional solar cell made on 243 cm^2 p-type silicon wafer. The n-type doped emitter layer is produced by diffusion of phosphorus using a tube furnace. The highly doped BSF layer is formed by alloying with an Al layer applied by screen-printing. A SiN_x layer is used for passivation and anti-reflective purposes on the front side of the solar cell. H-pattern metallisation on the front and three busbars on the rear are printed and fired to allow contacting and interconnection.

n-PERT solar cells (Czochralski-silicon, M0 wafers, 239 cm^2) are manufactured with standard processes on industrial tools as reported before [7,8]. Random pyramid texture is obtained with alkaline wafer etching. The diffused emitter and BSF are processed using industrial tube furnaces by Tempress [9]. The emitter is made using BBr_3 as precursor, the BSF is made using $POCl_3$ as precursor. The additional lateral conductivity in the phosphorus doped BSF contributes to a good FF despite the open rear side metallisation and increases the tolerance to high substrate resistivities. SiN_x layers for passivation and AR-coating purposes are deposited on the front and on the rear side. Screen or stencil printing can be used to apply the front and rear side metallisation grids. Both metallisation grids are fired in a single step in an IR-heated belt furnace.

Single-cell laminates were made by soldering tabs to the busbars of the solar cells. The cross-connected tabs on either side of the solar cell were contacted with two additional tabs to allow four-point measurements. Solar glass was used as front panel. Rear panel was either white back sheet or the same type of glass as on the front side. Fast-cure EVA was used as encapsulant.

Current-voltage (I-V) measurements have been conducted with a Class AAA solar simulator (Wacom) on a non-conductive, low reflective (anodised) chuck according to the IEC standard [10] under standard test conditions: 1000 W/m^2 with AM1.5 G spectrum, 25 °C. I-V measurements of the solar modules are measured by a category “class A” flash tester PASAN IIIb sun simulator, in accordance with IEC 60904-9.

Reflection and transmission of the cells, single-cell laminates and module materials are measured using the integrating sphere Labsphere RTC 060 SF. The wavelength range is 330–1750 nm. The reflection and transmission spectra are obtained by convolution of the relative reflection and transmission measurement with the reference AM1.5G spectrum. The absorption spectrum is calculated from the difference between the AM1.5G spectrum and the reflection and transmission spectra.

Spectral response is measured using a xenon lamp in combination with a filter wheel to excite the samples. Bias light is added to put the samples under testing in operational conditions. The filter wheel contains 32 optical band pass filters which have different wavelengths from 330 nm to 1200 nm.

The energy spectrum of the sum of the electrical power and the thermalisation, recombination, resistive and entropy generation losses is given by the convolution of the absorption spectrum with the IQE curve and the solar spectrum. The electrical power spectrum is this spectrum multiplied with the ratio $E_{g,mpp}$ / $E(\lambda)$, where $E_{g,mpp}$ is the energy corresponding to the maximum power point voltage and $E(\lambda)$ the energy of a photon with wavelength λ; the thermalisation spectrum with the ratio $(E(\lambda)\text{-}E_g)$ / $E(\lambda)$, with E_g the band gap energy of Si and the remaining loss spectrum with the ratio $(E_g\text{-}E_{g,mpp})$ / $E(\lambda)$. Finally, the parasitic heating is given by the absorption spectrum minus the power and loss spectra.

The outdoor measurement set-up consists of a south-facing tilted rack, that is open to the rear side. V_{oc}, I_{sc} and temperature of single-cell laminates were measured every 10 min in quick succession. To ensure the conditions are (nearly) identical for each measurement sequence, the in-plane irradiance was measured a few times before, in-between and after these single-cell measurements. In case the irradiance measurements within a sequence deviates too much, that data sequence was rejected. In-between the measurement sequences, all single-cell laminates were put under a passive load to mimic maximum power point conditions.

Also, the rooftop system on ECN.TNO's building was used to study the performance and actual temperature of commercial 60-cell modules. These measurements were also done in 10-min intervals, but all data and I-V curves were recorded simultaneously in 1 s. Details of that system have been reported before [11].

3. Results and discussion

3.1. Indoor characterisation to determine the heat input for solar cells

Two different cell architectures, including monofacial p-type Al-BSF and bifacial n-type PERT solar cells [12,13] were analysed using I-V, reflection, transmission and spectral response data. From these data, the spectral response of each cell over the AM1.5G spectrum is divided in generation of electric power, thermalisation, recombination and entropy generation losses, parasitic absorption and optical losses. Parasitic absorption includes free carrier absorption [5] and absorption by metal and module materials.

As example, the spectral analysis for an n-PERT solar cell is shown in Fig. 1. The thermalisation losses decrease steadily with increasing wavelength as the corresponding photon energy decreases towards the band gap energy of Si, i.e. 1.1 eV corresponding to 1100 nm. Consequently, at wavelengths above 1050 nm, near and above the bandgap, parasitic absorption becomes the dominant effect.

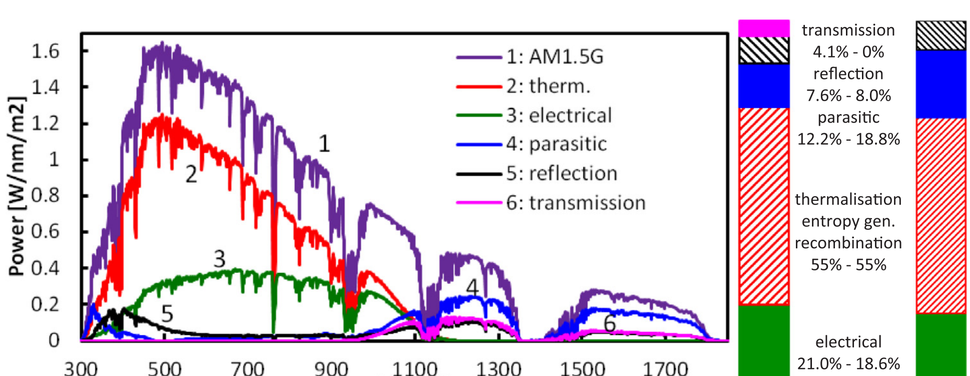

Fig. 1. Spectral distribution of electrical output and various loss mechanisms of an n-PERT solar cell; numbers in legend are used to distinguish the spectra. “therm.” Stands for the thermalisation, recombination and entropy generation losses. The bars on the right-hand show the relative parts of the total energy for an n-PERT and an Al-BSF solar cell; same colours are used in both graphs. (For interpretation of the references to color in this figure legend, the reader is referred to the web version of this article.).